

Wiley Geofluids Volume 2025, Article ID 6658750, 14 pages https://doi.org/10.1155/gfl/6658750



Research Article

Subsurface Gaseous Hydrocarbons and Carbon Dioxide Recorded During the Trans-Amazon Drilling Project (TADP) in the Acre Basin, Western Amazon

Angela Ethelis Jimenez Martinez D, André Oliveira Sawakuchi, Dailson José Bertassoli Júnior, Thomas Wiersberg, Siu Mui Tsai, Kleiton Rabelo de Araújo, Larissa Natsumi Tamura, Marcos Bolognini Barbosa, Tácio Cordeiro Bicudo, Alderlene Pimentel de Brito D, Ingo Daniel Wahnfried, Isaac Salém Azevedo Bezerra, Anders Noren, Cleverson Guizan Silva, Sherilyn Fritz, and Paul Baker

Correspondence should be addressed to Angela Ethelis Jimenez Martinez; angela_jimenez@usp.br

Received 31 March 2025; Revised 24 June 2025; Accepted 7 July 2025

Academic Editor: Fausto Grassa

Copyright © 2025 Angela Ethelis Jimenez Martinez et al. Geofluids published by John Wiley & Sons Ltd. This is an open access article under the terms of the Creative Commons Attribution License, which permits use, distribution and reproduction in any medium, provided the original work is properly cited.

The Trans-Amazon Drilling Project (TADP) drilled a sequence of claystones, siltstones, and sandstones in the Acre sedimentary basin, reaching a final depth of 923 m. This study characterizes the occurrence and compositional variation of light gaseous hydrocarbons detected using the online gas analysis (OLGA) monitoring system deployed during drilling, along with methane (CH₄) and carbon dioxide (CO₂) concentrations measured in discrete gas samples extracted from cores during drilling operations. The gaseous hydrocarbons detected by the OLGA system are predominantly CH₄ but with the regular presence of ethane (C₂H₆), propane (C₃H₈), isobutane (i-C₄H₁₀), and n-butane (n-C₄H₁₀). Zones with higher CH₄, C₂H₆, and C₃H₈ concentrations were observed at depth intervals of 250–380 and 420–588 m. These higher concentrations of CH₄, C₂H₆, and C₃H₈ occur in siltstone or sandstone layers capped by claystones, suggesting that these lithological associations act as stratigraphic gas traps. The Bernard parameter (CH₄/C₂H₆ + C₃H₈) varied from a low value of 2 at 466 m depth to a maximum value of 1904 at 621 m depth. Stable carbon isotope ratios of CH₄ show δ ¹³C values between –35‰ and –25‰, suggesting the nearly ubiquitous presence of thermogenic gas. The discrete gas samples from cores exhibited CO₂ concentrations between 230 and 1400 ppm in claystones, 850 and 950 ppm in siltstones, and 240–820 ppm in sandstone layers and from 2 to 4 ppm in siltstone and claystone layers. There is no significant correlation between CH₄ and CO₂ concentrations. These results provide evidence of light hydrocarbon migration from deeper thermally mature source rocks, with entrapment in sandstone layers capped by

¹Institute of Geosciences, University of São Paulo, São Paulo, São Paulo, Brazil

²GFZ Helmholtz Centre for Geosciences, Potsdam, Germany

³Cell and Molecular Biology Laboratory, Center for Nuclear Energy in Agriculture, University of Sao Paulo, Piracicaba, Brazil

⁴Universidade Federal do Amazonas, Manaus, Amazonas, Brazil

⁵Continental Scientific Drilling Facility, University of Minnesota, Minneapolis, Minnesota, USA

⁶Department of Geology and Marine Geophysics-LAGEMA, Institute of Geosciences, Fluminense Federal University, Niterói, Rio de Janeiro, Brazil

⁷Department of Earth and Atmospheric Sciences, University of Nebraska-Lincoln, Lincoln, Nebraska, USA

⁸Department of Earth and Climate Sciences, Duke University, Durham, North Carolina, USA

fine-grained sedimentary rock layers. The high concentration of CO_2 relative to CH_4 in fine-grained rock layers points to restricted conditions for microbial gas generation in the drilled sediments, possibly due to a combination of low organic carbon content and oxidizing conditions. This is in accordance with the abundance of reddish fine-grained paleosols in the drilled sedimentary units. The combination of online gas monitoring and discrete sampling methods allowed the comparison between gas collected during drilling and in situ gas, contributing to a better understanding of the processes of the subsurface carbon cycle.

Keywords: Amazon; drill-mud gas; fluvial deposits; gas migration; microbial methane; online gas analysis; Solimões Formation

1. Introduction

The Trans-Amazon Drilling Project (TADP) is aimed at reconstructing the Cenozoic evolution of the tropical South American climate, forests, mountains, and rivers to shed light on the origin of the Amazon biome [1]. Thus, scientific drilling with continuous coring was performed in the Acre and Marajó basins, respectively, in western and eastern lowland Amazonia. The TADP completed drilling (TADP-AC-1 well) in the Acre Basin in December of 2023, with continuous coring until a depth of 923 m. In addition to its paleoenvironmental and paleoclimatic goals, the TADP performed the first systematic gas geochemical investigation in the Acre Basin. This included the analysis of light hydrocarbons (C₁-C₄) and carbon dioxide (CO₂) during drilling, aimed at identifying microbial and thermogenic gas sources in the sedimentary column. Gas analyses were conducted using both real-time online gas analysis (OLGA) monitoring [2] and discrete sampling of pore gas from sealed drill cores.

Real-time gas monitoring of drilling fluids provides insights into gas flow and molecular composition, which are essential for understanding the generation and migration of hydrocarbons such as methane (CH₄), ethane (C₂H₆), propane (C₃H₈), isobutane (i-C₄H₁₀), and n-butane (n- C_4H_{10} [3–5]. While OLGA offers qualitative information on gas abundance, it enables the identification of permeable or sealing lithologies, aiding the reconstruction of hydrocarbon migration pathways and potential retention zones [6]. Additionally, molecular ratios (e.g., $CH_4/C_2H_6 + C_3H_8$, C_2H_6/C_3H_8 , and i- C_4H_{10}/n - C_4H_{10}) are used as proxies for gas origin and generation temperature [7, 8]. For instance, $CH_4/C_2H_6 + C_3H_8$ ratios > 1000 are indicative of microbial gas, while values < 100 suggest thermogenic origins. In parallel with the OLGA, discrete gas sampling was performed in cores during drilling. Thus, gas samples obtained from the headspace of sealed drill cores were further analyzed to obtain CH₄ and CO₂ concentrations as well as the CH₄ stable carbon isotope composition in discrete sedimentary rock

Here, we report data on light gaseous hydrocarbons and CO_2 recorded during drilling in the Acre Basin in the western Amazon. Gas concentration and composition variations in depth are discussed in terms of changes in sedimentary rock types and properties derived from the description of core catcher samples and downhole geophysical logging. CH_4 is recognized as a key greenhouse gas in the Earth's atmosphere [9]. While geological emissions have been recognized as a significant natural source of CH_4 to the atmosphere, with estimate ranging from 40 to 60 Tg yr⁻¹[10], recent studies have questioned the significance of these

emissions and their role in influencing global climate [11] Consequently, assessing the migration patterns and generation mechanism of both microbial and thermogenic CH₄ in sedimentary basins is essential for elucidating the relevance of geological sources of greenhouse gases.

2. The Acre Basin and the TADP-AC-1 Well

The Acre Basin in the lowland Amazon region, in the far west of Brazil (Figure 1b,c), covers an area of approximately 150,000 km² [12], of which around 40,000 km² includes buried Paleozoic rocks [13]. It is separated from the adjacent Solimões, Marañon, Ucayali, and Madre de Dios Basins by structural arches. Notably, the Acre Basin stands out in Brazil as the sole representative of a retroarc foreland basin type, directly impacted by Andean tectonics, showcasing well-defined Cenozoic fault systems and fold structures [14]. The Acre Basin had a multiphase long-term filling and comprises Paleozoic (Apuí, Cruzeiro do Sul, Rio do Moura Formations), Mesozoic (Juruá-Mirim, Moa, Rio Azul, Divisor Formations), and Cenozoic (Ramon and Solimões Formations) sedimentary rocks [15].

The Solimões Formation is characterized mostly by finegrained rocks (siltstones and claystones) and sandstones, with subordinate conglomerates and great lateral heterogeneities [13, 16-19], reaching up to 2200 m of thickness [13]. The upper Solimões Formation consists of interbedded sandstones and white-reddish claystones, while the lower portion, referred to as the Lower Solimões Formation, consists of claystone strata interbedded with siltstones, fine sandstones, and lignites, likely deposited in a reducing near-surface environment. The Solimões Formation has been assigned a Miocene age [20], but it can possibly reach the Pleistocene, with a depositional hiatus in the Pliocene [21]. Until 2000, 11 exploration wells were drilled in the Acre Basin. Three of these wells showed evidence of thermogenic hydrocarbon generation, indicating the existence of an active petroleum system [22, 23]. The well 1-RM-001-AC drilled by Petrobras found sediment layers with total organic carbon (TOC), with a maximum value of 6.45% [24] in the Permo-Carboniferous Cruzeiro do Sul Formation [24], which represents a potential deeper hydrocarbon source rock. No hydrocarbon shows were reported for Well 2-CDST1-AC (located about 0.6 km from our drill site) drilled through the Cruzeiro do Sul Formation and reached igneous basement rocks at ~2637 m depth. An east-west multichannel seismic line passing near the TADP-AC-1 drill site reveals nearly flat-lying strata. At depths below about 1000 m, reverse faults occur with minor vertical offset [23]. Elsewhere in the Acre Basin, surface geochemical studies

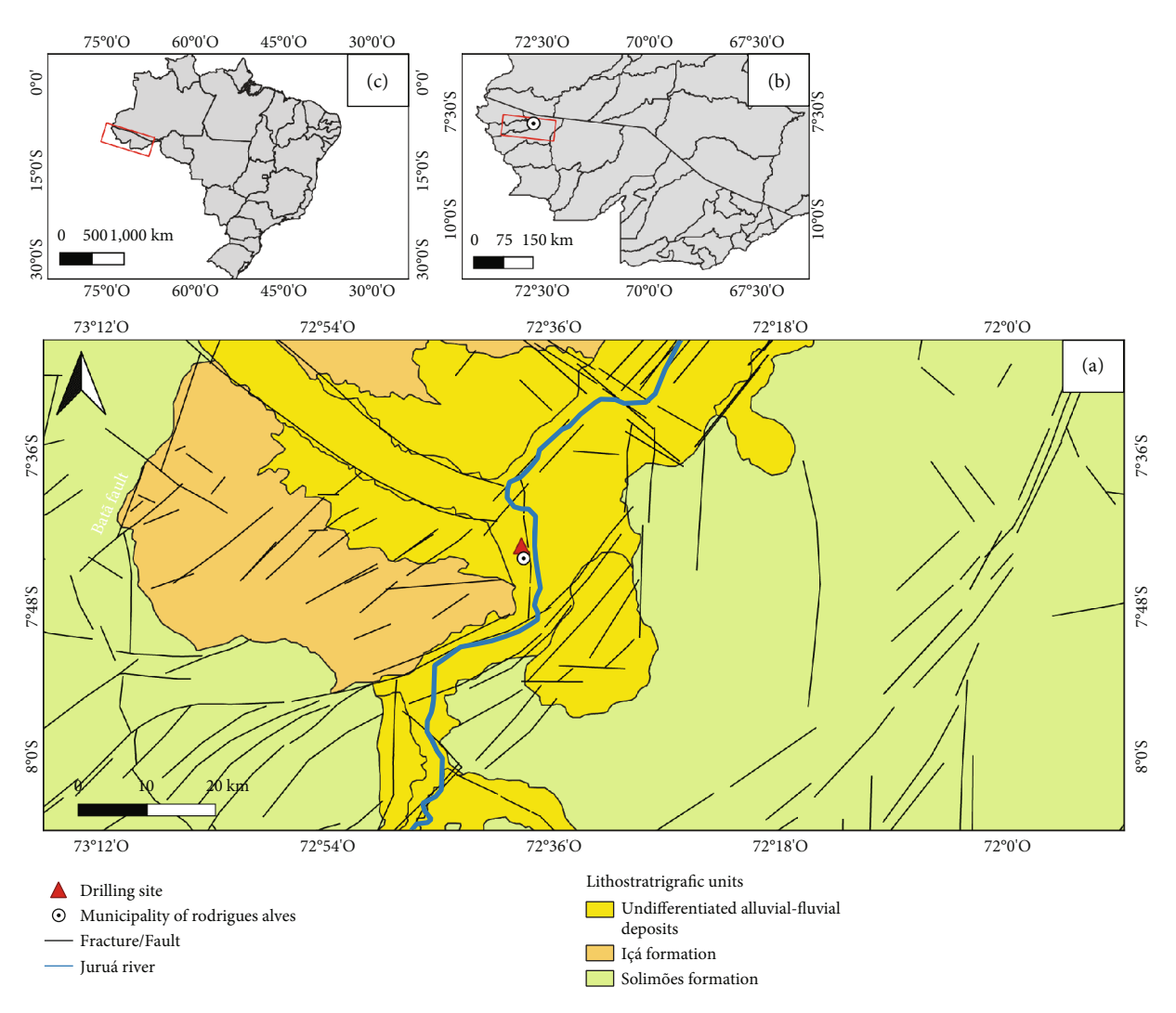


FIGURE 1: (a) Geological map of the Acre Basin showing the Cenozoic sedimentary cover and the location of the TADP-AC-1 drilling site in Rodrigues Alves, Acre State, Brazil. The undifferentiated alluvial–fluvial deposits correspond to Quaternary sediments accumulated in floodplains and low-elevation terraces. (b) Location of the municipality of Rodrigues Alves. (c) Location of Acre State within Brazil.

identified microseepages above and on the flanks of large magnetic highs, as well as along the traces of regional faults, indicating significant subsurface lateral and upward fluid movement with potential for hydrocarbons accumulation in upper sedimentary units of the Acre Basin, such as the Solimões Formation [13, 25, 26].

The TADP-AC-1 drilling site (07°43′42.01″ S//72°39′9.86″ O) is located ~700 m northwest of well 2CDST1AC and ~600 m west of the Juruá River in the municipality of Rodrigues Alves, Acre State (Figure 1a). The TADP-AC-1 drilling was executed using a Boart Longyear LF-230 drill rig (slim hole) operated by Geosol Geologia e Sondagens drilling company. Bentonite-based drilling fluid was used in Phase 1 of drilling (0–40 m depth), whereas cationic polymeric fluid was used in Phases 2, 3, and 4 (40–923 m depth). Drilling at the TADP-AC-1 site recovered 858.71 m of core, reaching a depth of 923.35 m (core recovery of 93%). Drilling Phase 1 reached 40 m depth with a core diameter of 8.3 cm and borehole enlargement to 31.11 cm for casing installation. Drilling with 8.3 cm (PQ) core diameter pro-

ceeded until 746 m depth (Phase 3), when it was reduced to a core diameter of 6.3 cm (HQ) until the final depth of 923 m (Phase 4).

3. Methods

3.1. OLGA During Drilling. Real-time OLGA of hydrocarbon gases (CH₄, C₂H₆, C₃H₈, n-C₄H₁₀, and i-C₄H₁₀) was conducted while drilling the TADP-AC-1 well. The OLGA uses a system consisting of a water–gas separator designed to mechanically extract gas dissolved in the drilling fluid [27, 28]. The degasser was placed in the drilling mud line outlet to ensure efficient gas extraction and minimize air contamination. The gas phase is continuously pumped through a 6-mm plastic tube (inner diameter: 4 mm) to the analytical laboratory that was located approximately 15 m from the drilling fluid circulation system (Figure 2). Hydrocarbons were analyzed continuously at 3-min intervals with a standard field automatic gas chromatograph (GC-SRI Instruments 86105400) equipped with a flame ionization detector

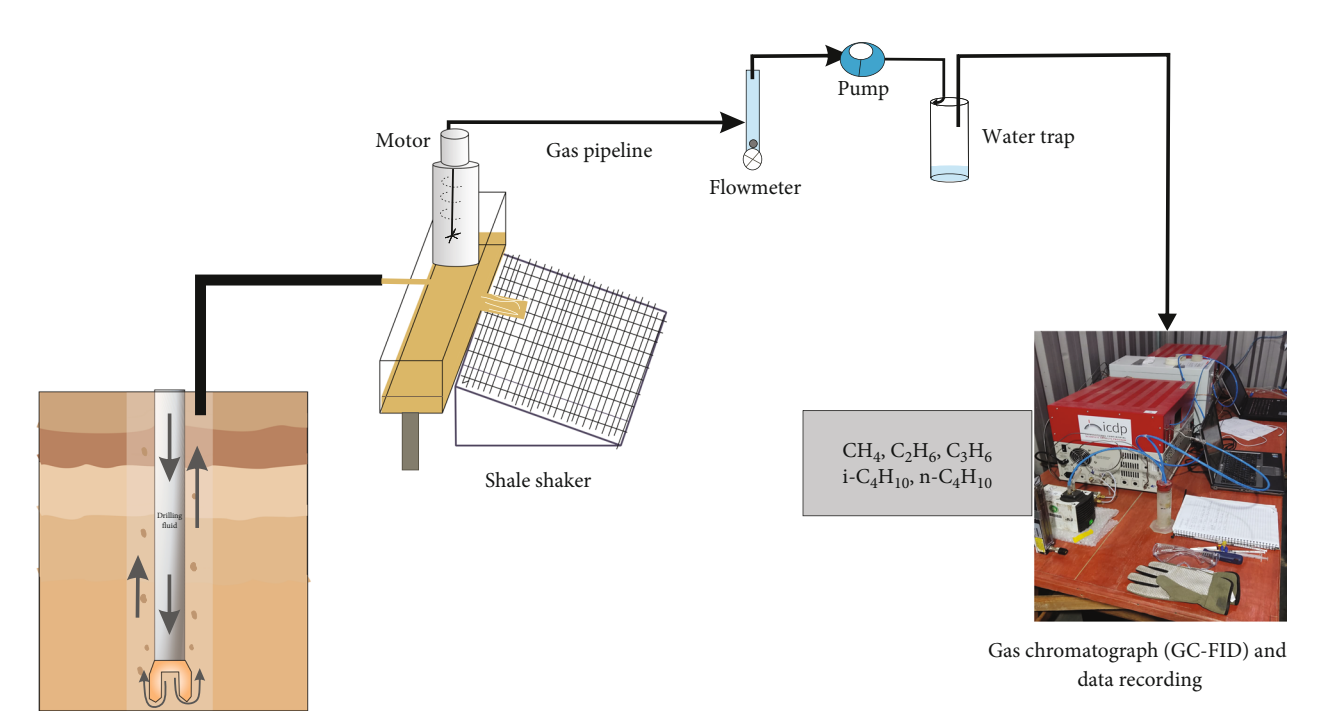


FIGURE 2: Schematic diagram of the gas monitoring system used during drilling of the TADP-AC-1 well. Gas released from the drilling fluid at the shaker is transported through a pipeline system that includes a water trap, pump, and flowmeter before reaching the gas chromatograph (GC-FID) for analysis. The system monitors light hydrocarbons represented by CH₄, C₂H₆, C₃H₈, i-C₄H₁₀, and n-C₄H₁₀.

(FID) and supported by a hydrogen generator (H2-100, SRI Instruments) device. The instrument was fitted with a $6' \times$ 1/8" OD stainless steel packed column. Hydrogen was used as the carrier gas at a flow rate of approximately 20 mL/min (regulated at 20 psi), and air was supplied at ~250 mL/min (5 psi) to sustain the flame. The detector temperature was set to 150°C, with FID gain set to "high" and the FID ignitor voltage at -750 V. The detection limit for light hydrocarbons (C_1-C_4) was approximately 0.1 ppm. Gas composition data were recorded over time. Depth of delay (lag depth) and penetration rate (ROP) provided by the drilling company allowed for the conversion of gas composition from drilling time to drilling depth. Instrument calibration was performed using standard gases with the following concentrations: CH_4 , 4870 ppm; C_2H_6 , 258 ppm; C_3H_8 , 200 ppm; $i-C_4H_{10}$, 99 ppm; and $n-C_4H_{10}$, 102 ppm, all with < 2% uncertainties.

3.2. Pore Gas Analysis During Drilling. Discrete gas samples were extracted directly from whole core sections using a headspace method. This allowed determination of the interstitial gas composition within specific sedimentary facies and depth intervals, thus avoiding possible mixing when gas is extracted from the drilling fluid circulation system. Interstitial gas was extracted from whole-core samples of 1–5 cm thickness, collected approximately every 20 m from 0 to 200 m depth and every 50 m below 200 m depth. The sampling intervals were chosen based on drilling operation constraints, such as core recovery, as well as the need to obtain representative gas samples across the sedimentary column. The core sample was stored in a gas-tight bag sealed with a manual heat sealer and then placed into a vacuum chamber for 30 min. Afterwards, a syringe of 5 cm³ (5 mL) volume

was used to extract a gas sample from the bag and to inject 1 mL into the sample inlet of a gas chromatograph (model SRI 8610 c) equipped with a FID detector [29, 30].

Below 550 m depth, an additional ~10 g sediment sample was collected from each core catcher for storage in a 60-mL glass vial, which was sealed with a septum. Ten milliliters of distilled water was added, and the vial was shaken for 3 min to release gases from the sedimentary rocks. The released gas was transferred to pre-evacuated glass vials, sealed with butyl rubber stoppers [30]. The gas samples were analyzed at the Institute of Geosciences of the University of São Paulo, using a gas chromatograph (TRACE 1310, Thermo Fisher Scientific) equipped with a loop injection system and an online methanizer coupled to a flame ionization detector (GC-FID) to identify and quantify CH₄ and CO₂. Readings were calibrated using a standard three-level calibration: (I) CH₄ at 1.519 ppm and CO₂ at 300 ppm, (II) CH₄ at 3.048 ppm and CO_2 at 2514 ppm, and (III) CH_4 at 50.59 ppm and CO₂ at 6007.00 ppm.

3.3. Analysis of CH₄ Stable Carbon Isotope. Gas samples with a volume of 25 mL were collected from the gas line when CH₄ concentrations exceeded 100 ppm, which occurred at drilling depths between 190 and 514 m. These samples were transferred into 12 mL Labco Exetainer vials for shipment and subsequent analysis. The stable carbon isotope composition (δ^{13} C) of CH₄ was determined at the Department of Plant Sciences, University of California, Davis, United States, following the method described by Yarnes et al. [31]. Analyses were performed using a Thermo Scientific GasBench II coupled with a PreCon trace gas concentration system and a Thermo Scientific Delta V Plus isotope-ratio mass spectrometer (IRMS).

Methane was cryogenically trapped and separated using a GS-Q column in dual LN₂ traps and then combusted to CO₂ in an alumina reactor containing NiO and Pt at 1000°C. Water was removed via a Nafion membrane prior to isotope measurement. Calibration procedures were applied identically to reference and sample materials and were directly traceable to the international standard VPDB for δ^{13} C.

3.4. Lithological Description. The texture and mineral composition of drilled lithologies were described on-site, under a binocular microscope, from core catcher samples. The depth frequency of the samples described varied according to each drilling maneuver, which reached up to 3 m. Five to ten grams was extracted from core catchers totaling 392 samples. This activity was performed by a sedimentologist as part of the on-site science team. This dataset was used to build a lithology column during drilling. The fragmented nature and small size of the core catcher samples hindered the descriptions of sedimentary structures.

3.5. Resistivity Downhole Logging. Resistivity downhole logging was performed with the model 40-GRP-1000 from Mount Sopris Instruments. This probe is capable of measuring resistivities ranging from 0.1 to 100,000 ohm-m, with an accuracy of less than 1% for values between 10 and 1000 ohm-m and less than 5% for values between 1 and 5000 ohm-m, and with a resolution of 0.04%. The operational principle is based on four electrodes, whose geometry of data acquisition allows investigation of the resistivity of two depths across the borehole wall. The first electrode at the top of the probe emits the current. The midway probe electrode measures resistivity 16 in. into the borehole wall (short normal), while another electrode at the base of the probe measures deeper resistivity, reaching 64 in. (long normal), possibly without or with minor influence of drilling fluid invasion. The last electrode is positioned far from the probe, acting as a reference and simulating electrical infinity compared to the other electrodes (spontaneous potential resistivity). Resistivity measurement was used to evaluate permeability, assuming that sedimentary facies with higher permeability exhibit significant contrast between short (N16) and long-distance (N64) resistivities due to drilling fluid invasion into the formation. The relative variation of resistivities recorded by short and long-distance curves also provides insight into natural fluid compositions, with higher long-distance resistivity values associated with lower salinity formation water or with the presence of hydrocarbons [32]. The resistivity downhole logging took place through the open hole from 40 to 557.45 m depth. The possibility of drill-pipe entrapment precluded open hole profiling in deeper portions of the borehole.

4. Results

4.1. Downhole Lithologies and Resistivities. The drilled sequence is composed of interbedded reddish claystone and reddish siltstones, along with grayish fine to mediumgrained sandstones. The sandstone layers, in particular, exhibit characteristics such as being friable, poorly cemen-

ted, and having a framework of moderately well-sorted rounded grains of fine sand. The claystone layers are mainly affected by intense mottling associated with heavy pedogenetic alterations.

Not surprisingly, sediments become increasingly consolidated with increased burial depth and age; however, even near the base of the core, many of the sandstones are weakly consolidated (Figure 3a). The entire drilled sequence is organized in stacked fining-upward cycles. In the interval from the surface to approximately 120 m depth, the finingupward cycle is composed primarily of thicker layers of medium sandstones, with high-frequency intercalations of fine-grained siltstones. The fining-upward cycles become thicker, as well as the claystones turning more frequent in the 125-260 m depth interval. Thicker intercalations of sandstone and claystone layers occur from 260 to 325 m depth. The 325-530 m depth interval is characterized by thicker claystone layers. Sandstone layers become thicker downhole and intercalated, mostly with claystones, until the 923 m depth. In the 540-750 m depth interval, the presence of fossil wood fragments (coal) was observed in the core catcher samples. Thicker claystone layers occur in the 720-745 and 870-890 m depth intervals.

Resistivity (short normal, long normal, and SPR) values are generally higher in sandstone intervals (Figure 3c). This is true for both short normal and long normal values, which track each other quite closely. Thicker sandstone layers show greater separation between short normal and long normal curves, as well as higher amplitude of variation in the SPR curve. This occurs, for example, at around 50, 100, and 300 m depth (Figure 3c). The long normal curve always recorded higher resistivity values compared to the short normal curve. The temperature profile across the studied depth interval ranges from 28°C to 34°C (Figure 3d.

4.2. OLGA Monitoring. The gas analyzed in the drilling fluid returns from the TADP-AC-1 well is dominated by CH₄, with minor concentrations of C₂H₆, C₃H₈, and n-C₄H₁₀. The continuous OLGA measurements identified several zones with higher concentrations of CH4 and variations in relative concentrations of CH₄, C₂H₆, C₃H₈, and i/n-C₄H₁₀ (Figure 4). Zones of higher CH₄ abundance occur at depths of 250–380 and 420–588 m (Figure 3b). The concentrations of C₂H₆ and C₃H₈ exhibit marked fluctuations, with notable peaks of both gases occurring at the same depths as those with higher CH₄ levels. By contrast, the concentrations of i-C₄H₁₀ and n-C₄H₁₀ are relatively lower in those intervals compared to CH₄, C₂H₆, and C₃H₈, with higher relative concentrations of i-C₄H₁₀ and n-C₄H₁₀ between 600 and 700 m (Figure 4). CH₄ exhibits a correlation of 0.34 (p > 0.05) with C_2H_6 , 0.38 (p > 0.05) with C_3H_8 , 0.43 (p > 0.05) with i- C_4H_{10} , and 0.43 (p > 0.05) with n- C_4H_{10} (Table 1). Additionally, C₂H₆ shows a strong correlation with C₃H₈, with a value of 0.85 (p > 0.05). Spearman correlations are considered significant when the p value is below 0.05, indicating that the observed relationship is unlikely due to random

Stable carbon isotopic analysis of eight samples of CH_4 taken from the gas line yields $\delta^{13}C$ values between -35%

6816, 2025, 1, Downloaded from https://onlinelibrary.wiley.com/doi/10.1155/gfl/6658750 by University Of Sao Paulo - Brazil, Wiley Online Library on [28/08/2025]. See the Terms and Conditions (https://onlinelibrary.wiley.com/terms-and-conditions) on Wiley Online Library for rules of use; OA articles are governed by the applicable Creative Commons License

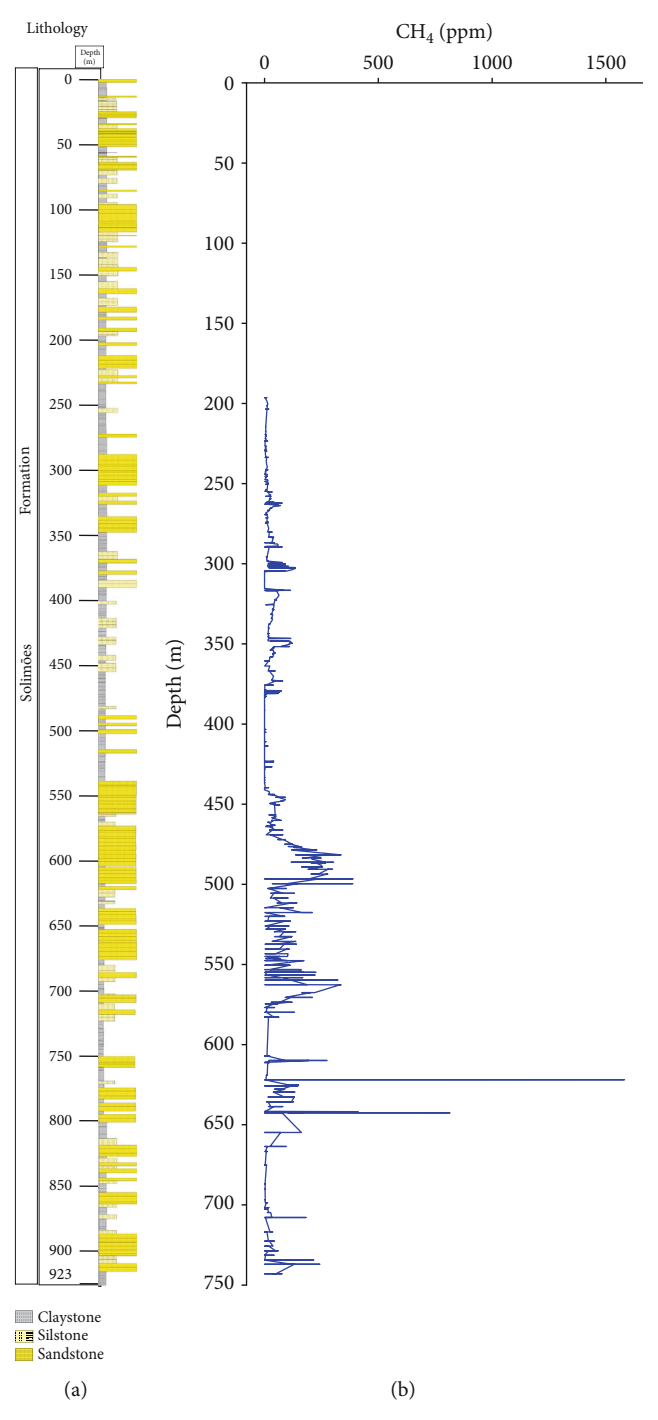


Figure 3: Continued.

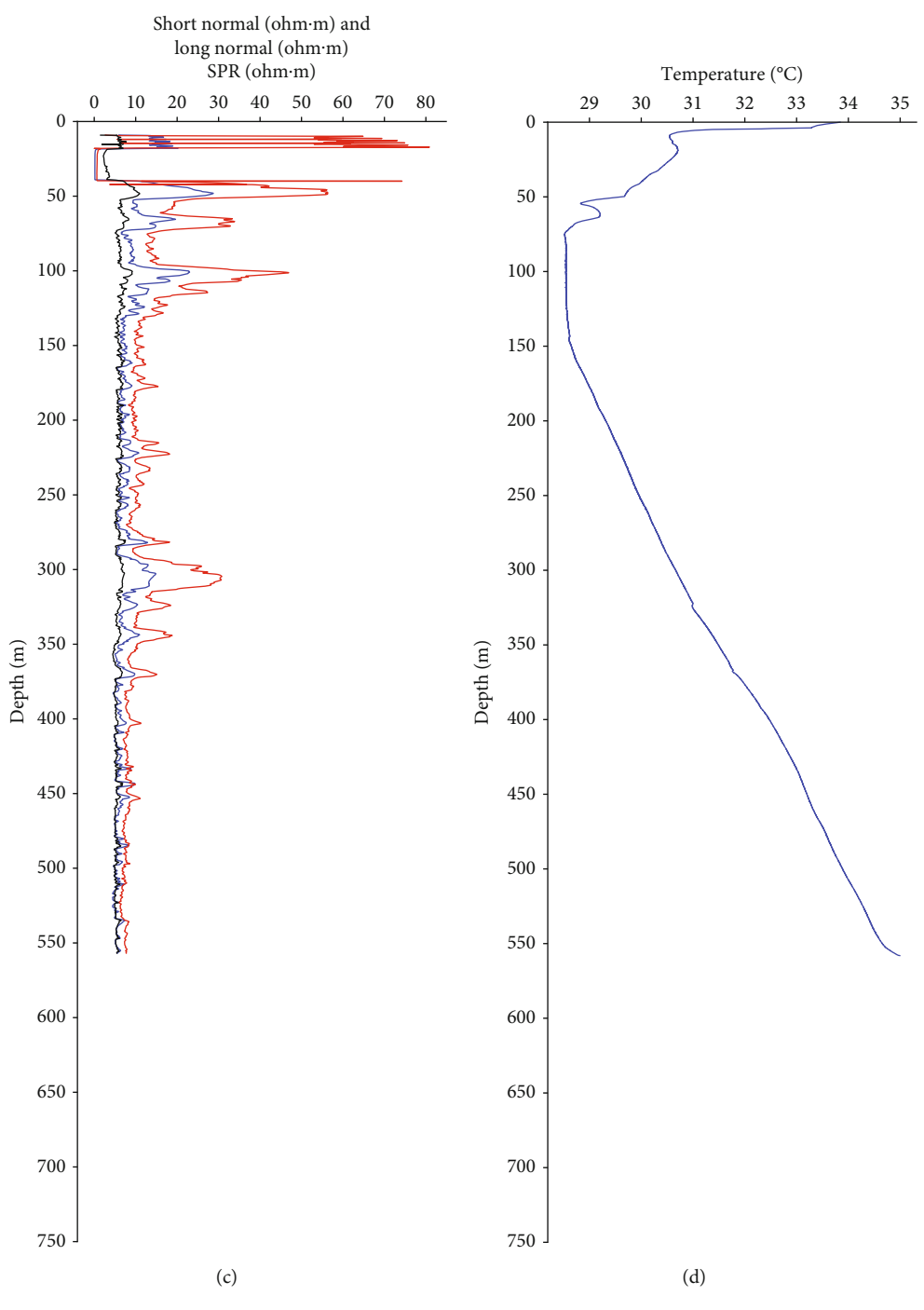


FIGURE 3: Comparison of lithology, CH_4 concentration, temperature, and resistivity from the TADP-AC-1 well between 0 and 758 m depth. (a) Lithological description based on core catcher samples. (b) Depth profile of CH_4 concentration in drilling mud obtained from online gas monitoring. (c) Resistivity logs (short normal, long normal, and SPR). (d) Temperature profile from the TADP-AC-1 well.

and -25% versus VPDB. The δ^{13} C in CH₄ was lower than -27% versus VPDB in the depth interval between 474 and 514 m. More negative δ^{13} C values were observed at depths from 300 to 314 m compared to other depth intervals (Figure 5b).

4.3. Measurements From Pore Gas Sampling. CH_4 concentrations in both discrete core samples and in the drilling fluid show similar variations (Figure 6a). In the samples between

50 and 750 m depth, CH_4 concentrations are low and show limited variation, whereas values are higher than 2 ppm below 580 m. The average atmospheric CH_4 concentration measured during drilling was 0.325 ± 0.003 ppm across four air samples. C_2H_6 , C_3H_8 , and i- C_4H_{10} have concentrations lower than 1 ppm and show peak concentrations in sediment samples below 500 m depth. In addition, as depth increases, C_2H_6 , C_3H_8 , and i- C_4H_{10} are detected in the pore gas samples. In the depth interval of 720–780 m (Figure 6b), CO_2

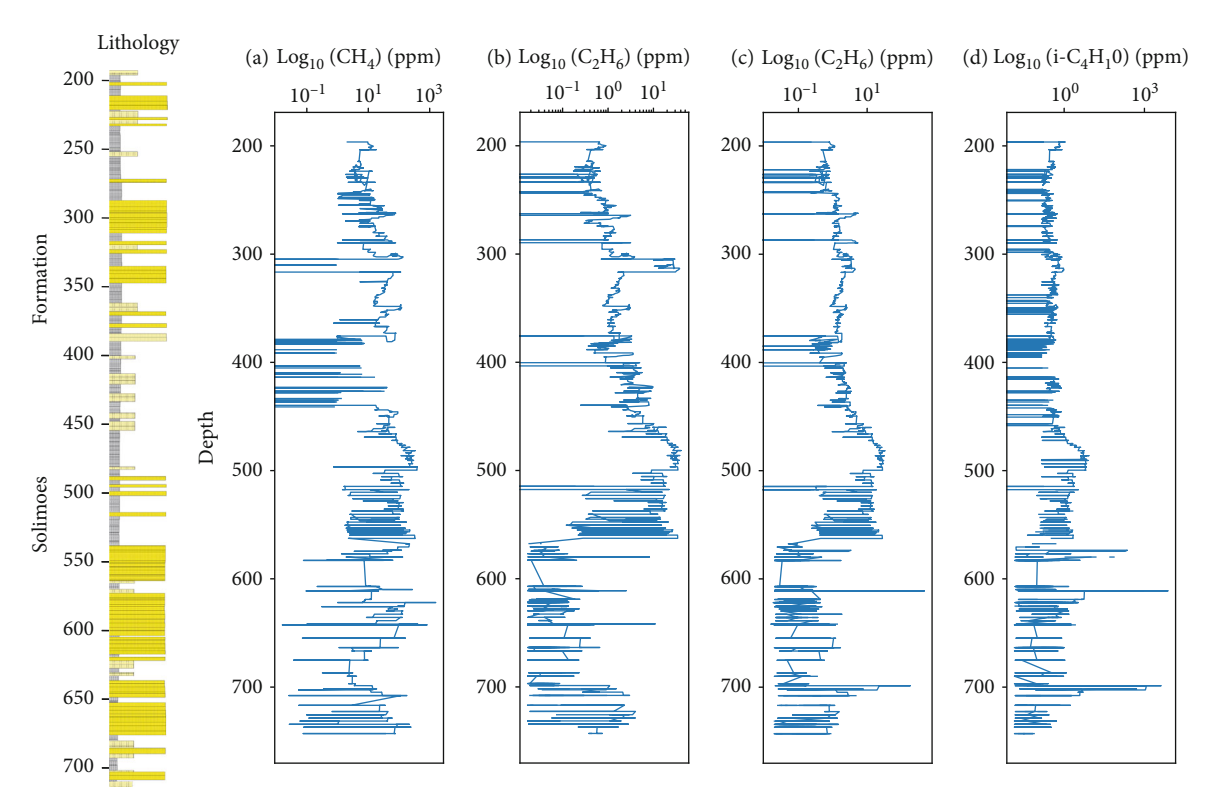


FIGURE 4: Depth profiles of CH_4 , C_2H_6 , C_3H_8 , $i-C_4H_{10}$, and $n-C_4H_{10}$ concentrations plotted on a semilogarithmic scale (log concentration (ppm) vs. depth (meter)), accompanied by lithological description based on core catcher samples from the TADP-AC-1 well.

TABLE 1: Spearman correlation coefficients between the concentrations of CH₄, C₂H₆, C₃H₈, and n-C₄H₁₀ measured using the online gas monitoring system during drilling of the TADP-AC-1 well. All correlations are significant at p < 0.05. A total of 11,070 measurements were performed between depths of 269 and 742.95 m.

Hydrocarbons	$\mathrm{CH_4}$	C_2H_6	C ₃ H ₈	i-C ₄ H ₁₀	n-C ₄ H ₁₀
CH4	1	0.3	0.38	0.44	0.27
C_2H_6		1	0.85	0.31	0.58
C_3H_8			1	0.43	0.74

concentrations range from 1632 to 182 ppm, with an average of 616.75 \pm 387.06 ppm. In the same interval, CH₄ concentration varies between 8.86 and 2.31 ppm, with an average of 3.54 \pm 1.5 ppm. At depths between 783 and 923 m, CO₂ concentrations range from 1290.47 to 239.48 ppm, with an average of 550 \pm 240 ppm (Figure 6c, while CH₄ ranges from 6.1 to 1.9 ppm, with an average of 2.73 \pm 0.73 ppm.

5. Discussion

The microbial degradation of organic matter in the subsurface contributes approximately 20% of global natural gas resources [33]. The remaining 80% originates from thermogenic gas, generated by the thermal cracking of organic matter when subjected to higher pressures and temperatures (>80°C) in the subsurface during burial in sedimentary basins [34, 35]. Microbial degradation primarily occurs in anoxic environments where organic matter is decomposed by methanogenic microbes (archaea) at lower temperatures,

producing microbial CH₄ [36, 37]. Both microbial and thermogenic gases can significantly impact the surface carbon cycle, because CH₄ may escape into the atmosphere if it is not oxidized by methanotrophic microorganisms before reaching the Earth's surface [38, 39]. Microbial CH₄ can be divided into two types based on its formation timing: (1) primary microbial biogenic CH₄, which is generated from the decomposition of recent organic matter, and (2) secondary microbial biogenic CH₄, which is produced when mature organic matter, such as kerogen, or its derived products, such as petroleum, are biodegraded by microorganisms after being exposed to groundwater [33]. While C₂ and C₃ hydrocarbons are thought to overwhelmingly arise from thermogenic decomposition (e.g., [40]), these gases can also be formed by relatively low-temperature, microbial processes [41], even in organic-poor sediments.

Given the relatively high δ^{13} C values of the discrete CH₄ samples, the parsimonious explanation for the origins of C₂H₆, C₃H₈, n-C₄H₁₀, and i-C₄H₁₀ that were observed in the core is that they were mainly products of the thermal decomposition of organic matter, reactions that were observed at depths and temperatures greater than ever witnessed by the present host sediment. According to the measurements, temperatures between depths of 0 and 578 m range from 28°C to 34°C, which would not be sufficient to generate these hydrocarbons through recent thermal processes. Thermogenic gases are generally characterized by higher concentrations of C₂+ hydrocarbons and by CH₄ with δ^{13} C values ranging from -50% to -30% versus VPDB [42, 43]. Microbial CH₄ produced in natural systems

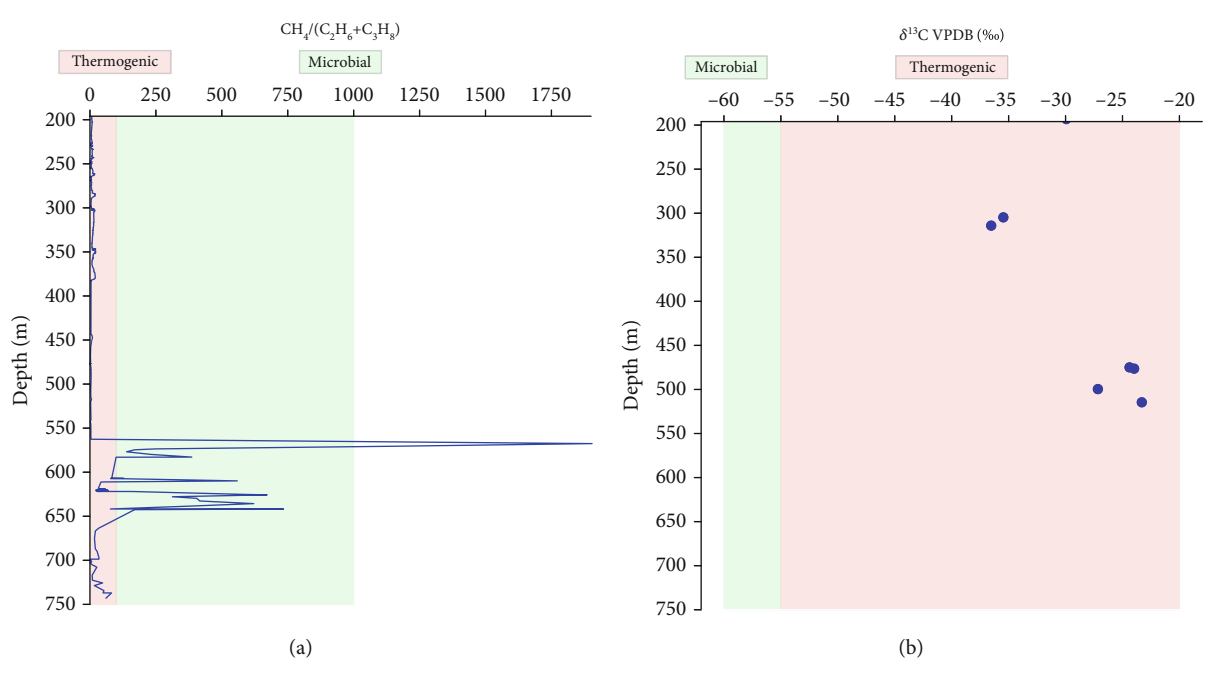


FIGURE 5: (a) Bernard parameter $CH_4/C_2H_6 + C_3H_8$ variation in the TADP-AC-1 well as an indicator of microbial and thermogenic gas origin. (b) Carbon stable isotope ($\delta^{13}C$) composition of CH_4 from the OLGA gas line plotted against drilling depth from the TADP-AC-1 well. Values higher than -55% are indicative of thermogenic sources, while values lower than -55% are indicative of microbial sources.

has δ^{13} C values ranging from -100% to approximately -55% versus VPDB, whereas the expected δ^{13} C range for thermogenic CH₄ is approximately -55% to -20% versus VPDB [39, 40, 44, 45].

In TADP-AC-1 well, the peaks of CH₄, C₂H₆, and C₃H₈ occur in layers of higher permeability rocks (sandstone). In the 540-750 m depth interval, a higher accumulation of gases (CH₄ and C₂H₆) was observed, with sandstone layers predominating. In the 540-921 m depth interval, the presence of fossil wood fragments (coal) was observed in the core catcher samples, suggesting a local source of microbial gas. A similar correlation between CH₄ distribution and layers containing coal and fossil wood fragments was observed during gas monitoring in the Kumano Basin during IODP NanTro-SEIZE Expedition 219 [46]. At a depth of 750 m, the presence of degraded heavy oil was observed, providing evidence of hydrocarbon migration. The Acre Basin shares similarities with foreland basins showing extensive and elongated depression formed by isostatic crustal subsidence due to the tectonic load imposed during a mountain building. This structural-stratigraphic geometry favors deep burial of eventually organic-rich sediments prone to the generation of thermogenic hydrocarbons, which can experience longdistance migration through continuous permeable sandy layers [47]. The thermally generated hydrocarbons can migrate laterally and upward along the inclined strata of permeable rocks connected with the source rocks, traveling several kilometers to structural and stratigraphic traps that are shallower and cooler, located at the basin margins [47]. Thus, light hydrocarbons detected in shallow sedimentary layers of the Acre Basin could be sourced by distant and deep buried organic-rich sediments, such as the Paleozoic shales of the Cruzeiro do Sul Formation. Vertical faults affecting the Acre Basin, such as the Batã Fault near the TADP-AC-1 drilling site, may also serve as potential vertical migration pathways for hydrocarbons. The Batã Fault is a prominent compressive structure located approximately 50 km east of the Divisor Fault, trending subparallel to it. It is interpreted that the Batã Fault originated during a Jurassic extensional deformation phase and was later inverted during the Andean orogeny [48]. The Batã Fault marks a notable deformation along the western margin of the Acre Basin, with most significant structures north of 9°S [26], where thicker sediment layers are preserved and fault-related folds may favor the trapping of hydrocarbons [12, 49].

Discrete pore gas samples obtained from the 500 to 600–700 m depth interval show a notable correlation among the CH₄, C₂H₆, and C₃H₈ concentrations, suggesting CH₄ of thermogenic origin. These gases are concentrated in sandstone layers interbedded with claystones and siltstones, according to the lithological descriptions from the core catchers. The sandstone layers, in particular, exhibit characteristics such as being friable, poorly cemented, and having a framework of moderately well-sorted rounded grains of fine sand. These sandstone properties can lead to high permeability, allowing gases like CH₄, C₂H₆, and C₃H₈ to accumulate and migrate more effectively through these layers compared to more compacted or less porous layers such as claystones.

In general, the drilled sequence of the Solimões Formation is composed of intercalations of sandstone, claystone, and siltstone layers, which provide extensive gas storage (sandstone) and seal (claystone or siltstone) capacity [50]. Microbial gas could be generated in organic-rich layers, usually represented by fine-grained sedimentary rocks such as claystones, migrating to those nearby sandstone layers that

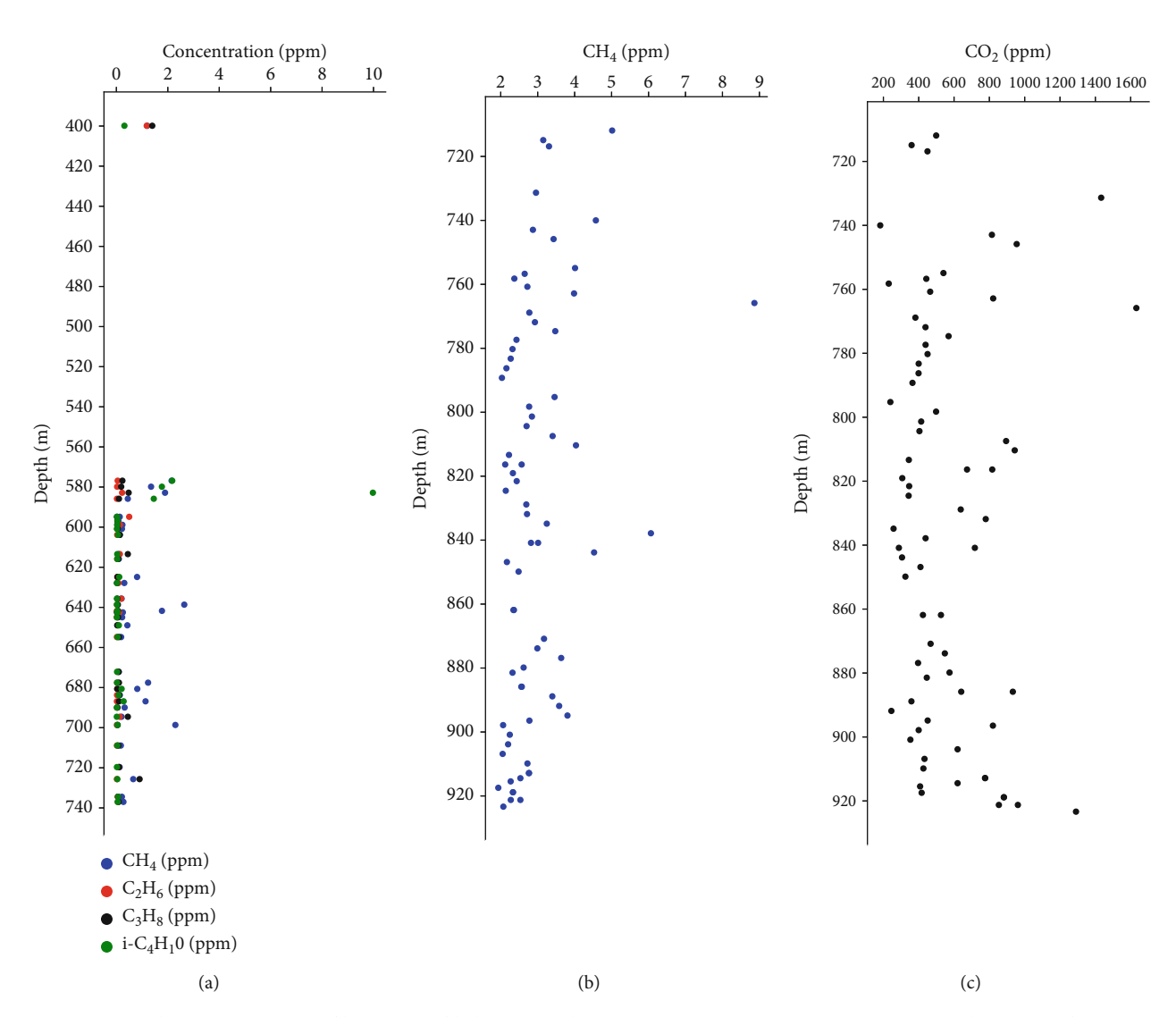


FIGURE 6: (a) Depth concentration profiles (ppm) of light gaseous hydrocarbons (CH_4 , C_2H_6 , C_3H_8 , i- C_4H_{10} , and n- C_4H_{10}) from pore gas samples collected in the TADP-AC-1 well, analyzed using a gas chromatograph (model SRI-8610) equipped with an FID detector. (b) CH_4 concentrations from pore gas samples. (c) CO_2 concentrations from pore gas samples. Profiles (b) and (c) were analyzed using a gas chromatograph (TRACE 1310, Thermo Fisher Scientific).

exhibit higher porosity (meso and macropores) and permeability [51]. These conditions could occur in the sedimentary layers drilled in the TADP-AC-1 well, as suggested by frequent intercalations of sandstones and claystones or siltstones. The presence of organic-rich claystone interbedded with highly porous and permeable sandstone creates the ideal conditions for the generation and migration of microbial gas in the subsurface [52, 53]. In the long normal resistivity profile (N-64) of the TADP-AC-1 well, higher resistivity was observed in the sandstone layers at depths of 295-310, 340-350, and 375-385 m. Deep resistivity measurement assesses the virgin zone that is relatively unaffected by drilling processes [54, 55]. Small amounts of gas can influence the long normal resistivity reading (Figure 3), depending on the quantity of gas and water salinity. High resistivity values are associated with the presence of free, that is, nondissolved gas in the formation [5], as gas is a nonconductive material, which increases the formation's resistivity.

However, this effect is dependent on gas solubility, which is controlled by gas concentration, pressure, temperature, and other factors, such as groundwater salinity.

The molecular ratios (Bernard parameters) of hydrocarbon gases typically vary within sedimentary basins [40, 56]. The $\mathrm{CH_4/C_2H_6+C_3H_8}$ ratio is a sensitive indicator of gas origin, often decreasing with increasing depth due to the increasing contribution of thermogenic gas with increasing depth and temperature [40, 57]. Ratios greater than ~1000 would indicate microbial gas generation, while ratios less than ~100 point to thermogenic gas origins [44, 58].

In the TADP-AC-1 well, the Bernard parameter showed values below 50 from the surface down to 466 m depth, indicating a strong influence of thermogenic gas in this interval. At 621 m, the maximum value of 1904 was recorded. To identify the $\mathrm{CH_4}$ origin (microbial vs. thermogenic), the carbon stable isotopic ($\delta^{13}\mathrm{C}$) composition of $\mathrm{CH_4}$ was analyzed both in gas samples collected from the drilling fluid and drill

cores. The analysis of δ^{13} C in CH₄ gives values lower than -27% PDB in the 474-514 m depth interval, suggesting a thermogenic origin [37]. At depths from 300 to 314 m, more negative values of δ^{13} C in CH₄ are observed compared to other depths. Changes in the isotopic composition of CH₄ may indicate different methanogenic pathways, such as a mixture of thermogenic and microbial methane or variations in the sources of carbon substrates [33, 59]. These isotopic variations may be associated with localized enrichment of organic matter, supported by the observation of plantderived carbon fragments in certain intervals of the formation. These plant residues can break down to generate ¹²Cenriched compounds like CO2 and acetate—key substrates for microbial methanogenesis [40]. Acetate is efficiently converted to CH₄ by methanogenic archaea [43, 60, 61]. Increased availability of these light carbon sources leads to more negative δ^{13} C-CH₄ values, which are typical of microbial methane production [61]. Additionally, the mixing of microbial and thermogenic gases could increase the proportion of CH_4 relative to C_2H_6 , producing more negative $\delta^{13}C$ values in CH₄ compared to the theoretical thermogenic endmember [62, 63]. The δ^{13} C values around -35%, observed at shallow depths (300-350 m) and moderate subsurface temperatures (~30°C) in the Acre Basin, suggest a mixed origin of CH₄, likely involving contributions from both earlymature thermogenic gas and secondary microbial CH₄. These intermediate isotopic signatures fall within the transition zone proposed by Milkov et al. [64], where microbial CH₄ generated during petroleum biodegradation can be enriched in 13 C (δ^{13} C between -40% and -30%). At such shallow depths, primary thermogenic gas generation is unlikely due to the absence of volcanic activity affecting the Acre Basin, but microbial activity is favored. This supports the interpretation that secondary microbial methanogenesis played a role in altering the original gas composition.

Similar δ^{13} C values and high $CH_4/(C_2H_6+C_3H_8)$ ratios (Figure 5a), as observed in the TADP-AC-1 well, have been reported in other sedimentary basins, such as in the Gulf of Mexico and North Carnarvon Basin [64, 65], where biodegradation and secondary microbial gas production are common. However, the drilled Solimões Formation in the Acre Basin presents distinctive features, including the persistence of isotopically mixed gases at very shallow depths and their stratigraphic association with fine-grained and/or organic-rich lithologies.

In the TADP-AC-1 well, a Spearman correlation index of 0.34 (p < 0.05) (Table 1) was obtained between CH₄ and C₂H₆, indicating a moderate positive relationship between these two hydrocarbon types. However, the relationship between CH₄ and C₂H₆ concentrations is not strong, suggesting that there may be other sources or factors influencing the presence of C₂H₆ in the composition of the Solimões Formation gases. Additionally, C₂H₆ can originate from thermogenic processes, as its concentration tends to increase with depth, suggesting a greater contribution of thermogenic gases in deeper layers [66]. However, the temperature variation in the drilled interval is minor, suggesting that the concentration of C₂H₆ is determined by migration and trapping controls. C₃H₁₀ showed a high and significant

correlation with C_2H_6 (0.846, p < 0.05) and $n-C_4H_{10}$ (0.737, p < 0.05), indicating a possibly similar source rock. As discussed, organic gases, represented by hydrocarbons and CO₂, generated by thermal degradation or biodegradation of organic matter could be produced in situ or migrate from a mature source at greater depths [3]. In the pore gas analysis, between depths of 720 and 920 m, CO₂ was detected, and although its concentration exhibited a weak positive correlation with CH₄ levels measured in the discrete samples (Spearman's $\rho = 0.1412$), this relationship was not statistically significant (p = 0.2438), indicating limited evidence of association between these gases. During the migration of thermogenic gas, CO₂ concentrations can be relatively high along with CH₄ [62, 63]. In contrast, in microbial degradation of organic matter, CO₂ produced by microbial processes or by the decomposition of organic matter can be incorporated into the methanogenic pathway, contributing to CH₄ generation in anoxic environments [42, 61].

The burial depth at the final depth of 923 m is unsuitable for reaching temperatures needed for the thermogenic generation of CH₄ or other gaseous hydrocarbons, which demand temperatures exceeding 70°C [66, 67]. Hence, the presence of thermogenic hydrocarbons in the well TADP-AC-1 points to hydrocarbon migration from deeper source rocks or exhumation of the Solimões Formation. Exhumation from burial depths reaching temperatures needed for thermogenic CH₄ to n-C₄H₁₀ generation would imply the erosive removal of a few kilometers of overlying sediments from the Miocene. This scenario is unsuitable considering the sedimentation ages attributed to the Solimões Formation [21]. Thus, hydrocarbon migration from greater depths and/ or over long horizontal distances is the most suitable explanation for the occurrence of thermogenic hydrocarbons in the upper portion of the Solimões Formation.

6. Conclusions

The analysis of gas composition obtained through continuous monitoring during drilling and discrete gas sampling in the TADP-AC-1 well in the Acre Basin provides insights into the geochemistry of subsurface fluids.

The distribution of CH_4 , C_2H_6 , C_3H_8 , and $i-C_4H_{10}$ aligns with the lithological characteristics of the drilled layers, particularly with sandstone and claystone layers, respectively, acting as gas storage and barrier migration layers, thus forming stratigraphic gas traps. A mixture of microbial and thermogenic CH₄ was detected, highlighting the presence of both shallow microbial activity and deeper thermal processes contributing to gas generation. However, there is a marked predominance of thermogenic gases over microbial gases, as indicated by the Bernard parameter and δ^{13} C in CH₄. The observed increase in C₂H₆, C₃H₈, and i-C₄H₁₀ concentrations with depth indicates that these sedimentary rocks contain minor amounts of migrated thermogenic hydrocarbons, consistent with the drilling site's location on the tapered eastern edge of the basin. Thermogenic gases would migrate from deeper layers and become trapped in sandstone layers with higher permeability. CH₄ released into the atmosphere, if not oxidized in the Solimões Formation

and overlying sediments, represents a potential contribution to the budget of climate-relevant gases to the atmosphere.

Regarding CO_2 , elevated and variable concentrations were observed in the deeper intervals (720–923 m), reaching up to 1632 ppm. Although the correlation between CH_4 and CO_2 was not statistically significant, the coexistence of both gases in organic-rich levels suggests the influence of microbial and/or thermogenic processes in the carbon cycle. These results highlight the importance of including CO_2 analysis in subsurface gas studies, particularly in tropical and underexplored settings such as the Acre Basin.

To improve the understanding of gas origin and migration processes in the Acre Basin, we recommend conducting complementary studies that include geochemical characterization of potential source rocks at greater depths, especially targeting intervals that may have reached sufficient thermal maturity to generate thermogenic hydrocarbons. Additionally, 3D basin modeling and hydrocarbon migration simulations could be employed to reconstruct possible migration pathways and evaluate the role of faults, stratigraphic discontinuities, and cap rocks in controlling gas distribution. These approaches will enhance the predictive capability regarding the origin, migration, and accumulation of natural gases in shallow formations such as the Solimões Formation.

Data Availability Statement

Data sharing is not applicable to this article as no new data were created or analyzed in this study.

Conflicts of Interest

The authors declare no conflicts of interest.

Funding

The study is funded by the Trans-Amazon Drilling Project through the International Continental Scientific Drilling Program (ICDP), the US National Science Foundation (1812681, 1812857, 1812541, 1812752, 1951112), the São Paulo Research Foundation (FAPESP) (2018/23899-2, 2023/00448-3), the Smithsonian Tropical Research Institute (STRI), the Fundação de Amparo à Pesquisa do Estado do Amazonas (FAPEAM) (Grant 01.02.016301.04190/2023-72—Universal Fapeam 20 Anos, 01.02.016301.04190/2023-72), and the Conselho Nacional de Desenvolvimento Científico e Tecnológico (CNPq) (421966/2023-8 CNPq/MCTI No. 10/2023). AOS is funded by CNPq (grant 307179/2021-4).

Acknowledgments

We greatly acknowledge the helpful support of the drilling operation team and science team engaged in the drilling operations of the TADP-AC-1 well. We are also grateful to the Rodrigues Alves municipality and its people for the kind and essential support during several steps of the drilling operations. The Federal University of Acre in Cruzeiro do Sul and Professor Francisco Ricardo Negri are thanked for

the essential support since the first steps of site surveys and planning of drilling operations.

References

- [1] P. A. Baker, S. C. Fritz, C. G. Silva, et al., "Trans-Amazon Drilling Project (TADP): Origins and Evolution of the Forests, Climate, and Hydrology of the South American Tropics," *Scientific Drilling* 20 (2015): 41–49, https://doi.org/10.5194/sd-20-41-2015.
- [2] J. Erzinger, T. Wiersberg, and E. Dahms, "Real-Time Mud Gas Logging During Drilling of the SAFOD Pilot Hole in Parkfield, CA," *Geophysical Research Letters* 31, no. 15 (2004): https://doi.org/10.1029/2003GL019395.
- [3] T. Wiersberg and J. Erzinger, "Origin and Spatial Distribution of Gas at Seismogenic Depths of the San Andreas Fault From Drill-Mud Gas Analysis," *Applied Geochemistry* 23, no. 6 (2008): 1675–1690, https://doi.org/10.1016/j.apgeochem.2008.01.012.
- [4] T. Wiersberg and J. Erzinger, "Chemical and Isotope Compositions of Drilling Mud Gas From the San Andreas Fault Observatory at Depth (SAFOD) Boreholes: Implications on Gas Migration and the Permeability Structure of the San Andreas Fault," *Chemical Geology* 284, no. 1-2 (2011): 148–159, https://doi.org/10.1016/j.chemgeo.2011.02.016.
- [5] T. Wiersberg, S. Pierdominici, H. Lorenz, B. Almqvist, I. Klonowska, and COSC Science Team, "Identification of Gas Inflow Zones in the COSC-1 Borehole (Jämtland, Central Sweden) by Drilling Mud Gas Monitoring, Downhole Geophysical Logging and Drill Core Analysis," *Applied Geochemis*try 114 (2020): 104513, https://doi.org/10.1016/ j.apgeochem.2019.104513.
- [6] S. Kotelnikova, "Microbial Production and Oxidation of Methane in Deep Subsurface," *Earth-Science Reviews* 58, no. 3-4 (2002): 367–395, https://doi.org/10.1016/S0012-8252(01)00082-4.
- [7] B. B. Bernard, J. M. Brooks, and W. M. Sackett, "Natural Gas Seepage in the Gulf of Mexico," *Earth and Planetary Science Letters* 31, no. 1 (1976): 48–54, https://doi.org/10.1016/0012-821X(76)90095-9.
- [8] E. Faber, W. J. Stahl, and M. J. Whiticar, "Distinction of Bacterial and Thermogenic Hydrocarbon Gases," in *Bacterial Gas: Proceedings of the Conference Held in Milan* (Editions Technip, 1992).
- [9] M. Etminan, G. Myhre, E. J. Highwood, and K. P. Shine, "Radiative Forcing of Carbon Dioxide, Methane, and Nitrous Oxide: A Significant Revision of the Methane Radiative Forcing," *Geophysical Research Letters* 43, no. 24 (2016): 12–614, https://doi.org/10.1002/2016GL071930.
- [10] G. Etiope, G. Ciotoli, S. Schwietzke, and M. Schoell, "Gridded Maps of Geological Methane Emissions and Their Isotopic Signature," *Earth System Science Data* 11, no. 1 (2019): 1–22, https://doi.org/10.5194/essd-11-1-2019.
- [11] B. Hmiel, V. V. Petrenko, M. N. Dyonisius, et al., "Preindustrial 14 CH₄ Indicates Greater Anthropogenic Fossil CH₄ Emissions," *Nature* 578, no. 7795 (2020): 409–412, https://doi.org/10.1038/s41586-020-1991-8.
- [12] R. V. A. Vasconcellos, R. L. Silveira, J. R. L. de Bezerrade, R. C. Alevato, and G. S. Barbosa, Bacia do Acre—Integração dos dados sísmicos e métodos potenciais adquiridos pela ANP (Anais, III Simpósio Brasileiro de Geofísica, Salinópolis, 2018), 1–4.
- [13] P. D. C. Cunha, "Bacia do Acre," Boletim de Geociências da Petrobras 15, no. 2 (2007): 207–215.

[14] M. R. Mello, 2009, e Elias, V. Estudo de Geoquímica e microbiologia de superfície na bacia do Acre. Relatório final de Projeto ANP-HRT. Rio de Janeiro, 109.

- [15] F. J. Feijo, R. G. de Souza, and A. Basin, "Bacia do Acre," Boletim de Geociencias da Petrobras 8 (1994).
- [16] M. Caputo, V. Rodrigues, and D. Vasconcelos, Litoestratigrafia da bacia do rio Amazonas (Relatório Técnico Interno 641) (p. 71, Petrobras-Renor, Rio de Janeiro.
- [17] M. Gross, W. E. Piller, M. I. Ramos, and J. D. da Silva Paz, "Late Miocene Sedimentary Environments in South-Western Amazonia (Solimões Formation; Brazil)," *Journal of South American Earth Sciences* 32, no. 2 (2011): 169–181, https://doi.org/10.1016/j.jsames.2011.05.004.
- [18] R. G. N. Maia, H. O. Godoyde, J. S. Yamaguti, et al., Projeto Carvão no Alto Solimões; Relatório final 1, Manaus, CPRM/ DNPM, 1977).
- [19] S. A. da Silva-Caminha, C. D'Apolito, C. Jaramillo, B. S. Espinosa, and M. Rueda, "Palynostratigraphy of the Ramon and Solimões Formations in the Acre Basin, Brazil," *Journal of South American Earth Sciences* 103 (2020): 102720, https://doi.org/10.1016/j.jsames.2020.102720.
- [20] C. D'Apolito, C. Jaramillo, and G. Harrington, *Miocene Palynology of the Solimões Formation (Well 1-AS-105-AM), Western Brazilian Amazonia* (Smithsonian Institution Scholarly Press, 2021).
- [21] C. A. Jaramillo, C. D'Apolito, S. A. F. Silva-Caminhada, and D. Caballero-Rodríguez, "A Palynological Zonation for the Neogene of the Solimões/Amazon Basin, Northwestern Amazonia," *Palynology* 49, no. 2 (2025): https://doi.org/10.1080/ 01916122.2024.2413153.
- [22] K. Cabral, Y. M. Muniz, N. J. R. Costa Junior, and Y. L. Fernandes, "Avaliação do potencial gerador da Formação Cruzeiro do Sul, Bacia do Acre, utilizando dados de pirólise rock-eval e carbono orgânico total," in *Congresso Brasileiro da Geologia* 49, SBG, 2018), http://cbg2018anais.siteoficial.ws/ST13/st13.htm.
- [23] R. V. A. Vasconcellos and C. I. Coutinho, 2013, Acre Basin. 12th Bidding Round of the ANP. Brazilian National Agency of Petroleum, Natural Gas and Biofuels (ANP).
- [24] ANP, "Brazilian Conventional Gas Reserves and Potential for Unconventional Gas," in *Seminar: Unconventional Gas* (BNDES, 2013), October 19, 2012. Retrieved from http://www.bndes.gov.br/SiteBNDES/bndes/bndes_pt/Institucional/Publicacoes/Paginas/s_gas_nao_convencional.html.
- [25] M. V. Caputo, "Juruá Orogeny: Brazil and Andean Countries," Brazilian Journal of Geology 44, no. 2 (2014): 181–190, https://doi.org/10.5327/Z2317-4889201400020001.
- [26] R. S. de Oliveira and R. M. Vidotti, "The Acre Basin Basement (NW Brazil) and the Transition From the Intracratonic to Retroarc Foreland Basin System," *Basin Research* 35, no. 1 (2023): 86–119, https://doi.org/10.1111/bre.12705.
- [27] J. Erzinger, T. Wiersberg, and M. Zimmer, "Real-Time Mud Gas Logging and Sampling During Drilling," *Geofluids* 6, no. 3 (2006): 225–233, https://doi.org/10.1111/j.1468-8123.2006.00152.x.
- [28] Z. Gong, H. Li, C. Lao, L. Tang, and L. Luo, "Real-Time Drilling Mud Gas Monitoring Records Seismic Damage Zone From the 2008 Mw7.9 Wenchuan Earthquake," *Tectonophysics* 639 (2015): 109–117, https://doi.org/10.1016/j.tecto.2014.11.017.
- [29] T. Hirose, M. Ikari, K. Kanagawa, G. Kimura, M. Kinoshita, and H. Kitajima, "Expedition 358 Methods," Proceedings of the International Ocean Discovery Program Expedition Reports

- 358, no. 102 (2020): https://doi.org/10.14379/iodp.proc. 358.102.2020.
- [30] T. D. Lorenson, M. J. Whiticar, A. Waseda, S. R. Dallimore, and T. S. Collett, Gas Composition and Isotopic Geochemistry of Cuttings, Core, and Gas Hydrate From the JAPEX/JNOC/ GSC Mallik 2L-38 Gas Hydrate Research Well (Bulletin-Geological Survey of Canada, 1999).
- [31] C. Yarnes, "δ ¹³C And δ²H Measurement of Methane From Ecological and Geological Sources by Gas Chromatography/Combustion/Pyrolysis Isotope-Ratio Mass Spectrometry," *Rapid Communications in Mass Spectrometry* 27, no. 9 (2013): 1036–1044, https://doi.org/10.1002/rcm.6549.
- [32] M. Rider, *The Geological Interpretation of Well Logs* (Gulf, Second edition, 2000).
- [33] D. S. Vinson, N. E. Blair, A. M. Martini, S. Larter, W. H. Orem, and J. C. McIntosh, "Microbial Methane From In Situ Biodegradation of Coal and Shale: A Review and Reevaluation of Hydrogen and Carbon Isotope Signatures," *Chemical Geology* 453 (2017): 128–145, https://doi.org/10.1016/j.chemgeo.2017.01.027.
- [34] D. D. Rice and G. E. Claypool, "Generation, Accumulation, and Resource Potential of Biogenic Gas," AAPG Bulletin 65, no. 1 (1981): 5–25, https://doi.org/10.1306/2F919765-16CE-11D7-8645000102C1865D.
- [35] D. D. Rice, J. L. Clayton, and M. J. Pawlewicz, "Characterization of Coal-Derived Hydrocarbons and Source-Rock Potential of Coal Beds, San Juan Basin, New Mexico and Colorado, U.S.A," *International Journal of Coal Geology* 13, no. 1-4 (1989): 597– 626, https://doi.org/10.1016/0166-5162(89)90108-0.
- [36] R. S. Hanson and T. E. Hanson, "Methanotrophic Bacteria," Microbiological Reviews 60, no. 2 (1996): 439–471, https://doi.org/10.1128/mr.60.2.439-471.1996.
- [37] M. J. Whiticar and E. Faber, "Methane Oxidation in Sediment and Water Column Environments—Isotope Evidence," *Organic Geochemistry* 10, no. 4-6 (1986): 759–768, https://doi.org/10.1016/S0146-6380(86)80013-4.
- [38] M. Formolo, "The Microbial Production of Methane and Other Volatile Hydrocarbons," in *Handbook of Hydrocarbon and Lipid Microbiology* (Springer, 2010).
- [39] E. R. Hornibrook and R. Aravena, "Isotopes and Methane Cycling," Environmental Isotopes in Biodegradation and Bioremediation 167 (2009): https://doi.org/10.1201/9781420012613.ch6.
- [40] S. D. Golding, C. J. Boreham, and J. S. Esterle, "Stable Isotope Geochemistry of Coal Bed and Shale Gas and Related Production Waters: A Review," *International Journal of Coal Geology* 120 (2013): 24–40, https://doi.org/10.1016/j.coal.2013.09.001.
- [41] K. U. Hinrichs, J. M. Hayes, W. Bach, et al., "Biological Formation of Ethane and Propane in the Deep Marine Subsurface," *Proceed*ings of the National Academy of Sciences 103, no. 40 (2006): 14684–14689, https://doi.org/10.1073/pnas.0606535103.
- [42] M. J. Whiticar, "Correlation of Natural Gases With Their Sources: Chapter 16: Part IV," *Identification and Characterization* 10 (1994): https://doi.org/10.1306/M60585.
- [43] M. J. Whiticar, "Carbon and Hydrogen Isotope Systematics of Bacterial Formation and Oxidation of Methane," *Chemical Geology* 161, no. 1-3 (1999): 291–314, https://doi.org/10.1016/S0009-2541(99)00092-3.
- [44] J. C. McIntosh, P. D. Warwick, A. M. Martini, and S. G. Osborn, "Coupled Hydrology and Biogeochemistry of Paleocene–Eocene Coal Beds, Northern Gulf of Mexico," *Bulletin* 122, no. 7-8 (2010): 1248–1264, https://doi.org/10.1130/B30039.1.

6816, 2025, 1, Downloaded from https://onlinelibrary.wiley.com/doi/10.1155/gf1.6658750 by University Of Soo Paulo - Brazil, Wiley Online Library on [28/08/2025]. See the Terms and Conditions (https://onlinelibrary.wiley.com/terms-and-conditions) on Wiley Online Library for rules of use; OA articles are governed by the applicable Certains Commons License

14 Geofluids

- [45] M. Schoell, "The Hydrogen and Carbon Isotopic Composition of Methane From Natural Gases of Various Origins," *Geochimica et Cosmochimica ACTA* 44, no. 5 (1980): 649–661, https://doi.org/10.1016/0016-7037(80)90155-6.
- [46] T. Wiersberg, A. M. Schleicher, K. Horiguchi, M. L. Doan, N. Eguchi, and J. Erzinger, "Origin and In Situ Concentrations of Hydrocarbons in the Kumano Forearc Basin From Drilling Mud Gas Monitoring During IODP NanTroSEIZE Exp. 319," *Applied Geochemistry* 61 (2015): 206–216, https://doi.org/ 10.1016/j.apgeochem.2015.06.002.
- [47] I. M. Head, D. M. Jones, and S. R. Larter, "Biological Activity in the Deep Subsurface and the Origin of Heavy Oil," *Nature* 426, no. 6964 (2003): 344–352, https://doi.org/10.1038/nature02134.
- [48] C. M. M. de Oliveira, P. V. Zalán, and F. F. Alkmin, "Tectonic Evolution of the Acre Basin, Brasil," VI Simpósio Bolivariano, Exploracion Petrolera en Las Cuencas Subandinas, Memórias, Tomo 1 (1997): 46–65.
- [49] P. Baby, Y. Calderón, C. Hurtado, et al., "The Peruvian Sub-Andean Foreland Basin System: Structural Overview, Geochronologic Constraints, and Unexplored Plays," in Petroleum Basins and Hydrocarbon Potential of the Andes of Peru and Bolivia, eds. G. Zamora, R. McClay, and V. A. Ramos (The American Association of Petroleum Geologists, 2018), 91–120, https://doi.org/10.1306/13622118M1173767.
- [50] Y. Dang, W. Zhao, A. Su, et al., "Biogenic Gas Systems in Eastern Qaidam Basin," *Marine and Petroleum Geology* 25, no. 4-5 (2008): 344–356, https://doi.org/10.1016/j.marpetgeo.2007.05.013.
- [51] Z. Chen, Y. Shuai, K. Osadetz, T. Hamblin, and S. Grasby, "Comparison of Biogenic Gas Fields in the Western Canada Sedimentary Basin and Qaidam Basin: Implications for Essential Geological Controls on Large Microbial Gas Accumulations," *Bulletin of Canadian Petroleum Geology* 63, no. 1 (2015): 33–52, https://doi.org/10.2113/gscpgbull.63.1.33.
- [52] M. Cokar, M. S. Kallos, H. Huang, S. R. Larter, and I. D. Gates, "Biogenic Gas Generation From Shallow Organic-Matter-Rich Shales," in *Proceedings of the SPE Canada Unconventional Resources Conference*, Article ID SPE-135323 (SPE, 2010).
- [53] N. Fishman, J. Neasham, D. Hall, and D. Higley, "Mudstone and Claystone Units: Seals for Ancient Microbial Gas Accumulations in the Upper Cretaceous Milk River Formation, Alberta and Saskatchewan," in Abstract for 2008 AAPG Annual Convention, San Antonio, Texas (AAPG, 2008).
- [54] O. E. Serra, Fundamentals of Well-Log Interpretation 1 (Elsevier Science Pub. Co., Inc., 1983).
- [55] O. E. Serra, Fundamentals of Well-Log Interpretation 2 (Elsevier Science Pub. Co., Inc., 1983).
- [56] D. D. Rice, "Composition and Origins of Coalbed Gas," Hydrocarbons from Coal: AAPG Studies in Geology 38, no. 1 (1993): 159–184, https://doi.org/10.1306/St38577C7.
- [57] J. M. Hunt, "Petroleum Geochemistry and Geology (Text-book)," in *Petroleum Geochemistry and Geology (Textbook)* (WH Freeman Company, 2nd edition, 1995).
- [58] B. B. Bernard, J. M. Brooks, and W. M. Sackett, "Light Hydrocarbons in Recent Texas Continental Shelf and Slope Sediments," *Journal of Geophysical Research: Oceans* 83, no. C8 (1978): 4053–4061, https://doi.org/10.1029/JC083iC08p04053.
- [59] D. Strapoć, M. Mastalerz, K. Dawson, et al., "Biogeochemistry of Microbial Coal-Bed Methane," *Annual Review of Earth and Planetary Sciences* 39, no. 1 (2011): 617–656, https://doi.org/ 10.1146/annurev-earth-040610-133343.

- [60] R. Conrad, "Quantification of Methanogenic Pathways Using Stable Carbon Isotopic Signatures: A Review and a Proposal," Organic Geochemistry 36, no. 5 (2005): 739–752, https://doi.org/10.1016/j.orggeochem.2004.09.006.
- [61] J. Penger, R. Conrad, and M. Blaser, "Stable Carbon Isotope Fractionation by Methylotrophic Methanogenic Archaea," Applied and Environmental Microbiology 78, no. 21 (2012): 7596–7602, https://doi.org/10.1128/AEM.01773-12.
- [62] P. D. Jenden, D. J. Drazan, and I. R. Kaplan, "Mixing of Thermogenic Natural Gas in Northern Appalachian Basin," AAPG Bulletin 77 (1993): 980–998, https://doi.org/10.1306/BDFF8DBC-1718-1.
- [63] B. Tilley and Muehlenbache, "Isotope Reversals and Universal Stages and Trends of Gas Maturation in Sealed, Self-Contained Petroleum Systems," *Chemical Geology* 339 (2013): 194–204, https://doi.org/10.1016/j.chemgeo.2012.08.002.
- [64] A. V. Milkov and G. Etiope, "Revised Genetic Diagrams for Natural Gases Based on a Global Dataset of >20, 000 Samples," Organic Geochemistry 125 (2018): 109–120, https://doi.org/ 10.1016/j.orggeochem.2018.09.002.
- [65] C. J. Boreham, D. S. Edwards, J. M. Hope, J. Chen, and Z. Hong, "Carbon and Hydrogen Isotopes of Neo-Pentane for Biodegraded Natural Gas Correlation," *Organic Geochemistry* 39, no. 10 (2008): 1483–1486, https://doi.org/10.1016/j.orggeochem.2008.06.010.
- [66] N. Mahlstedt, "Thermogenic Formation of Hydrocarbons in Sedimentary Basins," in *Hydrocarbons*, oils and lipids: Diversity, origin, chemistry and fate (Springer International Publishing, 2020), 493–522.
- [67] W. G. Darling, "Hydrothermal Hydrocarbon Gases: 1, Genesis and Geothermometry," *Applied Geochemistry* 13, no. 7 (1998): 815–824, https://doi.org/10.1016/S0883-2927(98)00013-4.